A Comprehensive 2D FE-SIBC Model for Calculating the Eddy Current Losses in a Transformer Tank-Wall

J. M. Díaz-Chacón, C. Hernandez, and M. A. Arjona

División de Estudios de Posgrado e Investigación
Instituto Tecnológico de la Laguna, Torreón, Coah. 27000, México
jmauri12@gmail.com, coni.hernandez@ieee.org, marjona@ieee.org

Abstract ─ The calculation of the eddy-current losses is one of the most important aspects that must be considered in the design of transformers and electrical machines. In this paper, a comprehensive 2D finite element (FE) model for calculating the eddy-current losses in a tank-wall of the transformer is presented. The FE model takes into account the Surface Impedance Boundary Condition (SIBC). A detailed 2D-SIBC formulation in terms of the magnetic vector potential is described. The SIBC is incorporated into the FE formulation by using the Galerkin method. An axi-symmetric electromagnetic model of the transformer is solved by applying the SIBC formulation for calculating the loss intensity distribution along the vertical tank-wall. To demonstrate the validity of the SIBC formulation, the results are compared against those computed with a model based on first-order triangular elements. The advantages of using the SIBC formulation in the modeling of power transformers are highlighted.

Index Terms – Eddy current losses, finite element method, power transformer, surface impedance boundary condition.

I. INTRODUCTION

The Finite Element Method (FEM) is a computational tool that can be applied in several fields of electrical engineering where knowledge of electromagnetic fields is needed [1]. Alwash et al. used the 3D-FEM to analyze a helical motion induction motor [2]. Afjei et al. applied the finite element (FE) in a switched reluctance generator under faulty conditions [3]. B. Ali et al. presented a 3D-FEM analysis in modeling periodic structures using high-order multiscalets functions [4]. Wan et al. implemented an efficient FE time-domain method via a hierarchical matrix algorithm for electromagnetic simulation [5]. Torkaman et al. applied the 3D-FEM to evaluate the main characteristics of a three-phase external rotor switched reluctance motor [6].

The power transformer is an essential component and the most expensive asset within the transmission and distribution electrical networks [7]. A transformer includes several metallic parts, such as frames, shunts, and the tank. In these metallic parts, the stray losses are generated by the magnetic flux leakage of the transformer windings. The prediction of the stray losses in the transformer is fundamental at the design stage. This can help to avoid the presence of hot spots on the surface of metallic components. In oil-immersed transformers, the appearance of hot spots may provoke an undesirable overheating of conductive regions. This may generate internal gases, which may lead to the transformer failure [8].

In conductive regions exposed to time varying electromagnetic fields where the penetration depth is much smaller than their domain size, the Surface Impedance Boundary Condition (SIBC) can be used to reduce the FE model size. Hence, the aim of combining the FEM and the SIBC is to reduce the computational cost needed in the solution of an eddy-current problem. The SIBC is

Submitted On: Jan. 6, 2012
Accepted On: July 22, 2012

based in the analytical solution of the diffusion equation. In FE transformer modeling, the computational cost to obtain stray losses in regions with induced eddy currents is high. This is due to the equipment size and the large number of finite elements needed in the discretisation of the metallic parts. Hence, the Surface Impedance Boundary Condition (SIBC) represents an economic alternative for calculating these stray losses because it avoids the FE meshing of conducting parts. The FE literature recommends the usage of line elements to represent the conductive regions with the SIBC [9-11]. For this reason, the incorporation of the SIBC into a FE model presents two important advantages in its usage. Firstly the resulting model decreases the computational cost and secondly it can easily be implemented into a FE code.

Several researchers have applied the SIBC for calculating the stray losses in power transformers. Holland et al. used 3D FE and SIBC to analyze the tank-wall losses of a three-phase transformer [12]. Guerin et al. made a simulation of a three-phase transformer using the volume AV, shell AV and surface impedance formulations [13]. Guerin et al. also applied the non-linear surface impedance condition using a B-H rectangular curve known as Agarwal curve to simulate an 100 MVA three-phase transformer [14].

In addition, some papers have published the application of the SIBC in electrical motors and in the time domain. Adamiak et al. analyzed a low-speed linear induction motor using the 2D SIBC [15]. Yuferev et al. presented several high order generalized expressions of the SIBC, which were obtained by solving the diffusion equation using a perturbation technique [16]. Sabariego et al. developed a dual formulation of the time-domain SIBC both the magnetic field and magnetic vector potential [17]. Sabariego et al. also combined the SIBC in the time domain with a coarse volume FE discretisation of the massive conductors to capture the slowly varying flux components [18].

Futhermore, the SIBC has also been applied to high frequencies problems. Sakellaris et al. developed a SIBC formulation based in the magnetic vector potential, which was applied to a high frequency problem [19]. Darcherif et al. applied the SIBC to obtain the parameters of multiconductor and shielded cables at medium and high frequencies [20].

However, the above references show a lack of a clarity in the SIBC formulation, which does not help to its implementation into a FE code. A FE beginner will grasp easily a detailed step-by-step SIBC formulation such that can be incorporated into his FE code. This can be useful in those situations where the usage of commercial software is not available due to its high cost.

In this paper, a comprehensive SIBC 2D-FE linear formulation is presented. This formulation is expressed in terms of the magnetic vector potential. To illustrate the SIBC application, an axi-symmetric model of the transformer is solved. The loss intensity on the vertical tank-wall of the transformer is obtained using the Poynting's vector formulation. The SIBC model is compared against the results of a first order FE model of the transformer. The results obtained demonstrate the validity of using the SIBC for calculating the stray losses on the tank-wall of a transformer.

II. FINITE ELEMENT DISCRETISATION

The diffusion equation can be derived from the Maxwell's equations. It describes the behavior of the electromagnetic fields in the frequency domain and it is given by [9].

$$\nu\nabla^2 A = j\omega\sigma A - J_0, \tag{1}$$

where ω is the angular frequency, σ and ν are the conductivity and reluctivity of the material, respectively. A is the magnetic vector potential. J_0 is the imposed current density.

The FEM can be used to obtain the solution to the diffusion equation in 2D. By applying the Galerkin method, where the residual is multiplied by a weighted function and by using first-order FE, the solution of (1) is given by (2) [19]:

$$\frac{\nu}{4\Delta}[S][A] + \frac{j\omega\sigma\Delta}{12}[T][A] = \frac{J_0\Delta}{3}[I], \tag{2}$$

where the matrices S and T are given by:

$$[S] = \begin{bmatrix} b_1^2 + c_1^2 & b_1b_2 + c_1c_2 & b_1b_3 + c_1c_3 \\ b_1b_2 + c_1c_2 & b_2^2 + c_2^2 & b_2b_3 + c_2c_3 \\ b_1b_3 + c_1c_3 & b_2b_3 + c_2c_3 & b_3^2 + c_3^2 \end{bmatrix}, \tag{3}$$

$$[T] = \begin{bmatrix} 2 & 1 & 1 \\ 1 & 2 & 1 \\ 1 & 1 & 2 \end{bmatrix}, [I] = \begin{bmatrix} 1 \\ 1 \\ 1 \end{bmatrix}, [A] = \begin{bmatrix} A_1 \\ A_2 \\ A_3 \end{bmatrix}. \tag{4}$$

Where b_1, b_2, b_3, c_1, c_2 and c_3 are geometrical coefficients and Δ is the area of the element. A_1, A_2 and A_3 are the nodal potentials on the element.

The calculation of the loss intensity P of a first-order FE is given by (5), (6) and (7) [21]

$$P = \mathrm{Re}\left\{\frac{JJ^*}{2\sigma}\right\}, \tag{5}$$

$$J = \sigma E, \tag{6}$$

$$E = -j\omega\frac{\left(A_1 + A_2 + A_3\right)}{3}, \tag{7}$$

where J is the eddy current density in a triangular element, J^* is its complex conjugate and E is the electric field.

III. THE SIBC FORMULATION

The SIBC has its origin in the phenomena known as skin effect, where the flux density is concentrated at the surface of the conductive material. This effect can be found in regions characterized by high values of permeability, conductivity or frequency. The diffusion equation without the presence of current sources is given by (8),

$$\nabla\times(\nabla\times\mathbf{A}) = j\omega\mu\sigma\mathbf{A}, \tag{8}$$

where μ is the permeability of the material.

The one-dimension (1D) form of (8) can be written as

$$\frac{\partial^2 A}{\partial x^2} = j\omega\mu\sigma A, \tag{9}$$

its analytical solution is given by (10) [10], and the normal derivative of the magnetic vector potential is given by (11).

$$A = A_0 e^{-\gamma x}, \tag{10}$$

$$\frac{\partial A}{\partial x} = \frac{\partial A}{\partial n} = -\gamma A_0 e^{-\gamma x} = -\gamma A, \tag{11}$$

where A_0 is the magnetic vector potential of the separating surface. γ and the penetration depth δ are defined by (12) and (13), respectively.

$$\gamma = \frac{1+j}{\delta}, \tag{12}$$

$$\delta = \sqrt{\frac{2}{\omega\mu\sigma}}. \tag{13}$$

To implement the concept of SIBC into a FE formulation, the diffusion equation is solved using the neighbor region jointed to the boundary with eddy currents [20].

$$\nabla\times(\nu_1\nabla\times\mathbf{A}) = 0, \tag{14}$$

where ν_1 is the reluctivity of the region without eddy currents.

By discretizing (14) with the FE Galerkin method and using the normal derivative (11) of the 1D analytical solution, the following result is obtained,

$$\nu_1\int_\Gamma N\frac{\partial A}{\partial n}\,d\Gamma = -\nu_2\gamma\int_\Gamma NA\,d\Gamma, \tag{15}$$

where ν_2 is the reluctivity of the region with eddy currents and N stands for the shape function.

Taking into account the right hand side of (15) and the linear interpolation of the potentials within a finite element, the expression (16) can be obtained,

$$-\nu_2\gamma\int_\Gamma NA\,d\Gamma = -\nu_2\gamma\int_\Gamma [N^e]^T[N^e][A^e]\,d\Gamma, \tag{16}$$

where $[N^e]$ are the shape functions of the linear element and $[A^e]$ are the unknown nodal potentials, which are expressed by (17) and (18). T means matrix transpose.

$$[N^e] = [N_1 \quad N_2], \tag{17}$$

$$[A^e] = \begin{bmatrix} A_1 \\ A_2 \end{bmatrix}. \tag{18}$$

Therefore, the discretisation of (16) of a linear element is as follows,

$$-\nu_2\gamma\int_\Gamma NAd\Gamma = -\nu_2\gamma\int_\Gamma \begin{bmatrix} N_1^2 & N_1N_2 \\ N_1N_2 & N_2^2 \end{bmatrix}\begin{bmatrix} A_1 \\ A_2 \end{bmatrix}d\Gamma. \tag{19}$$

By using the definite integral given in (20), the values of the characteristic matrix are obtained,

$$\int_\Gamma N_1^a N_2^b\,d\Gamma = \frac{a!b!l}{(a+b+1)!}, \tag{20}$$

where l is the length of the linear element and it is given by:

$$l = \sqrt{\left(x_1 - x_2\right)^2 + \left(y_1 - y_2\right)^2}, \tag{21}$$

where x_1, x_2, y_1 and y_2 are their spatial coordinates.

Therefore, Eq. (19) can be written as

$$-\nu_2\gamma\int_\Gamma NA\,d\Gamma = -\frac{\nu_2\gamma l}{6}\begin{bmatrix} 2 & 1 \\ 1 & 2 \end{bmatrix}\begin{bmatrix} A_1 \\ A_2 \end{bmatrix}. \tag{22}$$

Consequently, by employing the SIBC, the elemental matrix (2) can be transformed into:

$$\frac{\nu_1}{4\Delta}[S][A]+\frac{j\omega\sigma_1\Delta}{12}[T][A] +(1+j)\frac{\nu_2 l}{6\delta_s}[P][A]=\frac{J_0\Delta}{3}[I], \quad (23)$$

$$[P]=\begin{bmatrix}2 & 1 & 0\\ 1 & 2 & 0\\ 0 & 0 & 0\end{bmatrix}, \quad (24)$$

$$\delta_s=\sqrt{\frac{2\nu_2}{\omega\sigma_2}}. \quad (25)$$

Where σ_1 is the conductivity of the 2D region and σ_2 is the conductivity of the SIBC region.

The SIBC edge of the first-order FE is located between the first two local nodes, Fig. 1.

IV. APPLICATION OF THE SIBC TO A TRANSFORMER

This section presents the application of the SIBC for calculating the stray losses on the tank-wall of a transformer. The theory of Poynting's vector states that at the surface of good conductors the tangential components of the electric and magnetic fields are approximately proportional to each other. This is known as surface impedance [11].

The magnetic field intensity **H** within one FE is given by (26) [9]

$$\mathbf{H}=\nu_2\mathbf{B}=\nu_2\nabla\times\mathbf{u}_z A_0 e^{-\gamma x} =\mathbf{u}_y\nu_2\gamma A_0 e^{-\gamma x}=\mathbf{u}_y\nu_2\gamma A, \quad (26)$$

and the electric field **E** is expressed as (27).

$$\mathbf{E}=-j\omega\mathbf{A}=-\mathbf{u}_z j\omega A_0 e^{-\gamma x}=-\mathbf{u}_z j\omega A. \quad (27)$$

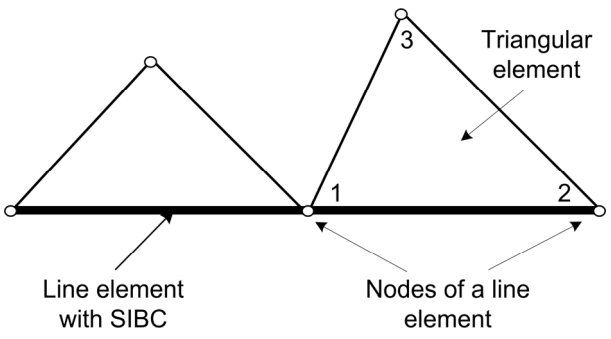

Fig. 1. Line element with SIBC between two first local nodes of a triangular element.

By employing (26) and (27), the surface impedance, Z_s, is obtained as (28).

$$Z_s=\frac{E_t}{H_t}=\frac{|\mathbf{E}|}{|\mathbf{H}|}=\frac{j\omega}{\nu_2\gamma}=\frac{\gamma}{\sigma_2}=\frac{(1+j)}{\sigma_2\delta_s}, \quad (28)$$

where E_t and H_t are the tangential components of the electric and magnetic fields, respectively.

Therefore the resulting equations for the post-processing of the solution are (29) and (30).

$$E_t=-j\omega\frac{(A_1+A_2)}{2}, \quad (29)$$

$$H_t=\frac{E_t\sigma_2\delta_s}{\sqrt{2}}. \quad (30)$$

The loss intensity P_e within a linear element is obtained by using the Poynting vector and it is given by (31).

$$P_e=\frac{1}{2}\mathrm{Re}(Z_s)|H_t|^2=\frac{1}{2}\frac{|H_t|^2}{\sigma_2\delta_s}. \quad (31)$$

The SIBC formulation is implemented in a C language program and the solver PARDISO is used to solve the resulting system of linear equations [22-23].

For a student, the demonstration of the validity of the SIBC formulation is illustrative. For this purpose, two FE meshes of the axi-symmetric model of the transformer (Fig. 2) are constructed. The loss intensity along the vertical tank-wall is calculated by employing two FE meshes. One mesh is generated using first-order FE to represent the tank-wall while the other mesh is created using line elements that represent the SIBC. The thickness of the tank-wall is 4.83 mm. The parameters of the transformer model are shown in Table 1 and the electrical frequency is 60 Hz. Therefore, the skin depth has a value of 1.2579 mm which is smaller than the thickness of the tank-wall. The FE meshes were generated using a free software library [24]. A computer with an Intel dual-core processor was used in the simulations. The mesh size and the computational time for each model are indicated in Table 2. It can be seen that by using the SIBC approach, the mesh size can be reduced by 57.44 % and the computational time can be decreased by 52.34 %.

The comparative results of eddy current losses by using the SIBC and FE used to represent the plate of transformer tank-wall are shown in Table 3.

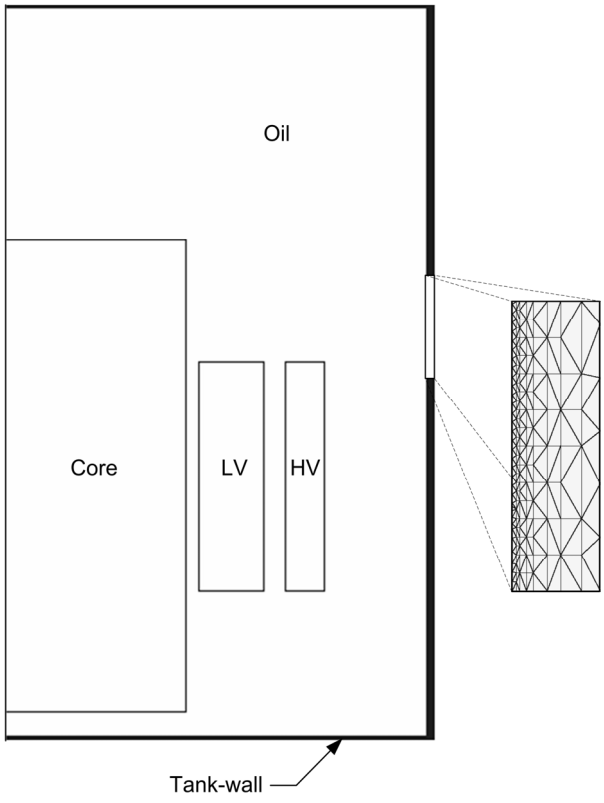

Fig. 2. Schematic diagram of the transformer FE model.

It can be seen that both results are almost of the same magnitude. This demonstrates the validity of the SIBC formulation. Table 3 also shows that losses are mainly concentrated in the vertical tank wall due to the small loss increment obtained in the total stray losses.

The flux distribution obtained with the model that uses first-order FE is shown in Fig. 3, whereas the solution obtained by using the SIBC formulation is illustrated in Fig. 4. It can be seen that both flux distributions are very similar.

In order to compare the loss intensity on the vertical tank-wall, it is firstly computed with a first-order FE mesh. A technique was developed to obtain this surface representation of loss intensity. This technique is based on the linear distribution property of losses within a FE. Firstly, the total area of the vertical tank-wall is divided into equidistant rectangular regions. This allows the calculation of loss intensity by using the loss quantity allocated in each rectangular region. An interpolation technique was used to obtain the amount of the losses in the rectangular area.

Table 1: Parameters of the transformer model

Region	Current	Turns	μ_r	σ
LV	5552.3A	6.0	1.0	—
HV	53.56 A	622.0	1.0	—
Core	—	—	Non-linear (M4)	0.0 S
Oil	—	—	1.0	0.0 S
Tank	—	—	400.0	6.67e6 S

Thereafter, the losses of each rectangular region are divided along its vertical length (height). Since the problem is axi-symmetric, the losses are also divided by its cylindrical depth, $2\pi r$, where r is the radius of the tank-wall surface. To illustrate the above process, a mesh with six rectangular regions (shaded) is shown in Fig. 5. To complement the analysis presented in this paper, the magnetic nonlinearity of the tank-wall material is included in the FE model. The Newton-Raphson algorithm is employed to solve the resulting nonlinear equations. The A36 steel is used to represent the tank-wall. The loss intensity behavior in the transformer tank-wall is shown in Fig. 6. It can be observed that the nonlinear model underpredicts the loss intensity with respect to the linear FE and SIBC-FE models. This is a useful result for manufacturers because a linear solution can be used to approximately predict the eddy current losses. The rather small loss difference is due to the slightly saturation of the transformer plates since it is only excited by the magnetic leakage fluxes of the transformer windings.

Table 2: CPU time and mesh size for both models

Model	CPU time	Nodes
Linear FE	40.92 s	278,249
Linear SIBC-FE	21.42 s	160,018
Non-linear FE	253.81 s	278,249

Table 3: Computed stray losses of the transformer

Model	Vertical tank-wall losses	Total tank-wall losses
Linear FE	84.3245 W	86.9237 W
Linear SIBC-FE	84.5805 W	87.1889 W
Non-linear FE	77.5774 W	79.2268 W

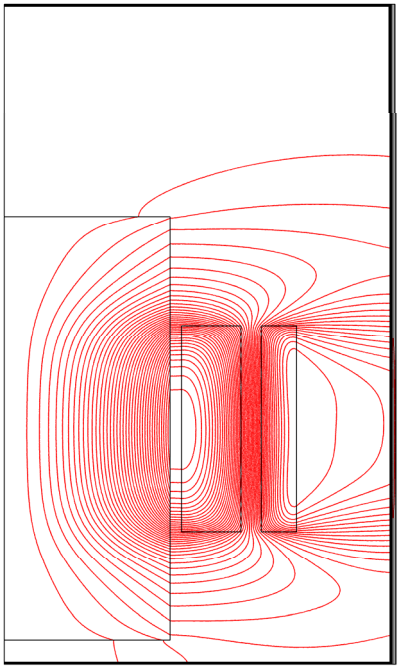

Fig. 3. Flux distribution in the FE linear model of the transformer.

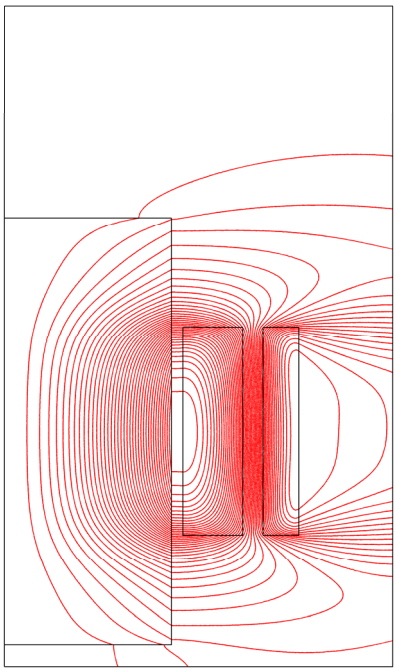

Fig. 4. Flux distribution in the SIBC-FE linear model.

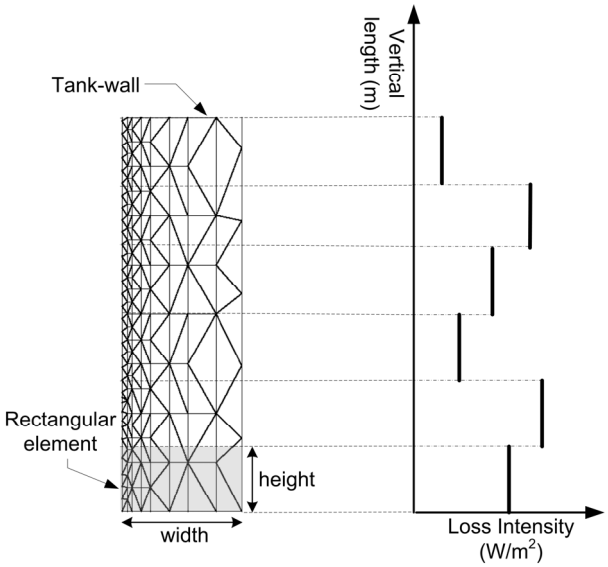

Fig. 5. Projection of the FE losses in the vertical tank-wall into an equivalent surface.

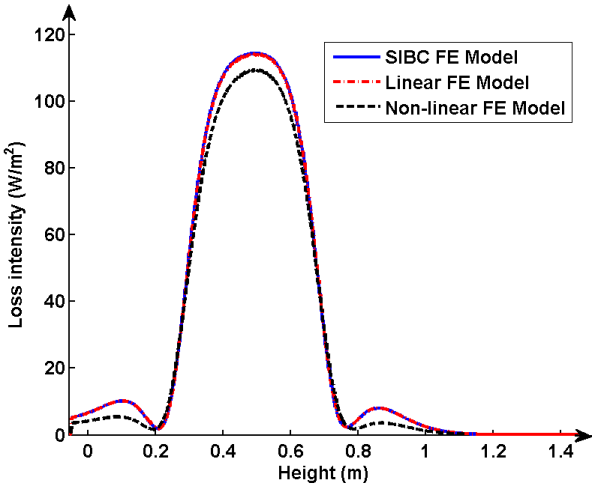

Fig. 6. Loss intensity behavior along the vertical tank-wall.

V. CONCLUSION

In this paper, a comprehensive FE-SIBC formulation has been presented and applied to the modeling of the transformer tank-wall. The formulation allows an easy understanding of the SIBC and its incorporation into a FE code. Besides, it was illustrated that this formulation has advantages in terms of computational time and mesh size, which makes it attractive for computing stray losses in large electrical equipment. An axi-symmetric FE model of the transformer was

developed and the SIBC formulation was used to represent the tank-wall. In order to compare the results obtained by using the SIBC and FE models, a projection technique of the 2D-FE losses was developed. Finally, it was shown that the SIBC is a useful approach that can be used in conductive regions allowing to decrease the FE mesh size.

ACKNOWLEDGMENT

The authors would like to thank to CONACYT, PROMEP and DGEST for their financial support to carry out this work.

REFERENCES

[1] S. Savin, S. Ait-Amar, D. Roger, and G. Vélu, "Prospective method for partial discharge detection in large AC machines using magnetic sensors in low electric field zones," *Applied Computational Electromagnetics Society (ACES) Journal*, vol. 26, no. 9, pp. 729-736, September 2011.

[2] J. H. Alwash and L. J. Qaseer, "Three-dimension finite element analysis of a helical motion induction motor," *Applied Computational Electromagnetics Society (ACES) Journal*, vol. 25, no. 8, pp. 703-712, August 2010.

[3] E. Afjei and H. Torkaman, "Finite element analysis of switched reluctance generator fault condition oriented towards diagnosis of eccentricity fault," *Applied Computational Electromagnetics Society (ACES) Journal*, vol. 26, no. 1, pp. 8-16, January 2011.

[4] A. B. Ali, E. A. Hajlaoui, and A. Gharsallah, "Efficient analysis technique for modeling periodic structures based on finite element method using high-order multiscalets functions," *Applied Computational Electromagnetics Society (ACES) Journal*, vol. 25, no. 9, pp. 755-763, September 2011.

[5] T. Wan, R. Cheng, J. She, D. Ding, and Z. Fan, "An efficient finite-element time-domain method via hierarchical matrix algorithm for electromagnetic simulation", *Applied Computational Electromagnetics Society (ACES) Journal*, vol. 26, no. 7, pp. 584-595, July 2011.

[6] H. Torkaman, N. Arbab, H. Karim, and E. Afjei, "Fundamental and magnetic force analysis of an external rotor switched reluctance motor," *Applied Computational Electromagnetics Society (ACES) Journal*, vol. 26, no. 10, pp. 868-875, October 2011.

[7] S. V. Kulkarni and S. A. Khaparde, *Transformer Engineering Design and Practice*, Marcel Dekker, Inc. New York, 2004.

[8] S. Singh and M. N. Bandyopadhyay, "Dissolved gas analysis technique for incipient fault diagnosis in power transformers: A bibliographic survey," *IEEE Electrical Insulation Magazine*, vol. 26, no. 6, pp. 41-46, November/December 2010.

[9] S. R. H. Hoole, *Computer Aided Analysis Design of Electromagnetic Devices*, Elsevier, New York, 1989.

[10] K. J. Binns, P. J. Lawrenson, and C. W. Trowbridge, *The Analytical and Numerical Solution of Electric and Magnetic Fields*, John Wiley & Sons, London, 1994.

[11] S. V. Yuferev and N. Ida, *Surface Impedance Boundary Conditions: A Comprehensive Approach*, CRC Press, 2010.

[12] S. Holland, G. P. O'Connell, and L. Haydock, "Calculating stray losses in power transformers using surface impedance with finite elements," *IEEE Trans. on Magnetics*, vol. 28, no. 2, pp. 1355-1358, March 1992.

[13] C. Guerin, G. Tanneau, and G. Meunier, "3D eddy current losses calculation in transformer tanks using the finite element method," *IEEE Trans. on Magnetics*, vol. 29, no. 2, pp. 1419-1422, March 1993.

[14] C. Guerin and G. Meunier, "Surface impedance for 3D non-linear eddy current problem - application to loss computation in transformers," *IEEE Trans. on Magnetics*, vol. 32, no. 3, pp. 808-811, May 1996.

[15] K. Adamiak, G. E. Dawson, and A. R. Eastham, "Application of impedance boundary conditions in finite element analysis of linear motors," *IEEE Trans. on Magnetics*, vol. 27, no. 6, Part: 2, pp. 5193-5195, November 1991.

[16] S. Yuferev and L. Di Rienzo, "Surface-impedance boundary conditions in terms of various formalisms," *IEEE Trans. on Magnetics*, vol. 46, no. 9, pp. 3617-3628, September 2010.

[17] R. V. Sabariego, P. Dular, C. Geuzaine, and J. Gyselinck, "Surface-impedance boundary conditions in dual time-domain finite-element formulations," *IEEE Trans. on Magnetics*, vol. 46, no. 8, pp. 3524-3531, August 2010.

[18] R. V. Sabariego, C. Geuzaine, P. Dular, and J. Gyselinck, "Time-domain surface impedance boundary conditions enhanced by coarse volume finite-element discretisation," *IEEE Trans. on Magnetics*, vol. 48, no. 2, pp. 631-634, February 2012.

[19] J. Sakellaris, G. Meunier, A. Raizer, and A. Darcherif, "The impedance boundary condition applied to the finite element method using the magnetic vector potential as state variable: a rigorous solution for high frequency axisymmetric

problems," *IEEE Trans. on Magnetics*, vol. 28, no. 2, pp. 1643-1646, March 1992.

[20] A. Darcherif, A. Raizer, J. Sakellaris, and G. Meunier, "On the use of the surface impedance concept in shielded and multiconductor cable characterization by the finite element method," *IEEE Trans. on Magnetics*, vol. 28, no. 2, pp. 1446-1449, March 1992.

[21] S. J. Salon, *Finite Element Analysis of Electrical Machines*, Springer, 1995.

[22] O. Schenk and K. Gartner, "Solving unsymmetric sparse systems of linear equations with PARDISO," *Journal of Future Generation Computer Systems*, vol. 20, pp. 475-487, 2004.

[23] O. Schenk and K. Gartner, "On fast factorization pivoting methods for symmetric indefinite systems," *Elec. Trans. Numer. Anal.*, vol. 23, pp. 158-179, 2006.

[24] J. R. Shewchuk, "Triangle: engineering a 2D quality mesh generator and Delaunay triangulator," *Applied Computational Geometry: Towards Geometric Engineering*, *Lectures notes in Computer Science,* Springer-Verlag Berlin, vol. 1148, pp. 203-222, May 1996.

J. M. Díaz-Chacón received the B.Sc. degree in electronic engineering in 2006 and M.Sc. degree in electrical engineering in 2010 from the Instituto Tecnológico de la Laguna, Torreón, México. He is currently working toward his doctoral degree in electrical engineering at the Instituto Tecnológico de la Laguna. His research interests include numerical methods applied to analysis of electrical machines.

C. Hernandez received the B.Sc. degree in computer science from the Instituto Tecnológico de Estudios Superiores de Monterrey, Monterrey, México, in 1990, the M.Sc. degree in foundations of advanced information technology from Imperial College, London, U.K., in 1995, and the Sc.D. degree in electrical engineering from the Instituto Tecnológico de la Laguna, Torreón, México, in 2007. She was with the Simulation Department, Instituto de Investigaciones Eléctricas from 1991 to 2000. She is currently with the Instituto Tecnológico de la Laguna, Torreón, México. Her interests are in artificial intelligence and global optimization applied to electrical machines.

M. A. Arjona received the B.Sc. degree in electrical engineering from the Instituto Tecnológico de Durango, Durango, México, in 1988, the M.Sc. degree in electrical engineering from the Instituto Tecnológico de la Laguna, Torreón, México, in 1990, and the Ph.D. degree in electrical engineering from Imperial College, London, U.K., in 1996.

He was with the Simulation Department, Instituto de Investigaciones Eléctricas from 1991 to 1999. He is currently a Professor of electrical machines with the Instituto Tecnológico de la Laguna. His interests are in the electromagnetic design, analysis, and control of electrical machines.